Available online at www.sciencedirect.com
SCIENCE DIRECT®
Atmospheric Environment 39 (2005) 5363–5374
ATMOSPHERIC ENVIRONMENT
www.elsevier.com/locate/atmosenv

Fine structure of mass size distributions in an urban environment

Imre Salma[a,*], Rita Ocskay[a], Nico Raes[b], Willy Maenhaut[b]

[a]*Eötvös University, Environmental Chemistry, H-1518 Budapest, P.O. Box 32, Hungary*
[b]*Ghent University, Institute for Nuclear Sciences, Proeftuinstraat 86, B–9000 Ghent, Belgium*

Received 16 December 2004; received in revised form 18 May 2005; accepted 25 May 2005

Abstract

As part of an urban aerosol research project, aerosol samples were collected by a small deposit area low-pressure impactor and a micro-orifice uniform deposit impactor in downtown Budapest in spring 2002. A total number of 23 samples were obtained with each device for separate daytime periods and nights. The samples were analysed by particle-induced X-ray emission spectrometry for 29 elements, or by gravimetry for particulate mass. The raw size distribution data were processed by the inversion program MICRON utilising the calibrated collection efficiency curve for each impactor stage in order to study the mass size distributions in the size range of about 50 nm to 10 μm in detail. Concentration, geometric mean aerodynamic diameter, and geometric standard deviation for each contributing mode were determined and further evaluated. For the crustal elements, two modes were identified in the mass size distributions: a major coarse mode and a (so-called) intermediate mode, which contained about 4% of the elemental mass. The coarse mode was associated with suspension, resuspension, and abrasion processes, whereby the major contribution likely came from road dust, while the particles of the intermediate mode may have originated from the same but also from the other sources. The typical anthropogenic elements exhibited usually trimodal size distributions including a coarse mode and two submicrometer modes instead of a single accumulation mode. The mode diameter of the upper submicrometer mode was somewhat lower for the particulate mass (PM) and S than for the anthropogenic metals, suggesting different sources and/or source processes. The different relative intensities of the two submicrometer modes for the anthropogenic elements and the PM indicate that the elements and PM have multiple sources. An Aitken mode was unambiguously observed for S, Zn, and K, but in a few cases only. The relatively large coarse mode of Cu and Zn, and the small night-to-daytime period concentration ratio pointed to anthropogenic sources by disintegration, which were related to vehicular traffic, i.e., mechanical wear of brake linings and tires, respectively.

Keywords: Cascade impactor; Inversion; Size distribution; Modal parameters; Element; PM

1. Introduction

There is an increased scientific interest in both climate forcing (Jacobson, 2001; Kaufman et al., 2002; Penner et al., 2004; Crutzen, 2004) and health effects (HEI, 2002; Pope et al., 2002; Balásházy et al., 2003) of atmospheric aerosols since several years. Key aerosol properties in this respect are the size distribution and chemical composition as a function of size and time. In addition, the size distributions provide valuable information on the sources and source processes and on the

*Corresponding author. Tel.: +36 1 372 26 15.
E-mail address: salma@para.chem.elte.hu (I. Salma).

1352-2310/$ - see front matter © 2005 Elsevier Ltd. All rights reserved.
doi:10.1016/j.atmosenv.2005.05.021

transformation processes during atmospheric transport, and are required for estimating the dry deposition of the aerosols. Consequently, the mass or number size distributions of particulate matter (PM), elements, main ions, and carbonaceous constituents have been studied in great detail (e.g., Morawska et al., 1999; Vignati et al., 1999; Offenberg and Baker, 2000; Allen et al., 2001; Hillamo et al., 2001; Maenhaut et al., 2002; Singh et al., 2002; Wehner and Wiedensohler, 2003; Pakkanen et al., 2003; Berner et al., 2004; Hussein et al., 2004; and references cited therein). Nevertheless, increased size resolution of modern cascade impactors and some developments in their calibration (Hillamo and Kauppinen, 1991; Maenhaut et al., 1996) combined with advanced mathematical algorithms for processing the experimental data (Wolfenbarger and Seinfeld, 1990; Talukdar and Swihart, 2003) give new possibilities for determining the overall shape of the mass size distributions in detail, i.e., the fine structure of the size distributions.

Within an urban aerosol research project, aerosol samples were collected by several filter-based devices and cascade impactors, and some on-line (in situ) aerosol measurements were performed in downtown Budapest, Hungary, in spring 2002 in the non-heating season in order to perform comprehensive physico-chemical characterisation of particulate organic matter (OM), elemental carbon (EC) and inorganic species (Salma et al., 2004; Maenhaut et al., 2005). The study is a follow-up and complement to our earlier investigations (e.g., Salma et al., 2001; Salma et al., 2002). The median PM concentration was found to be 30 and 20 $\mu g\,m^{-3}$ for the PM10–2.0 and PM2.0 size fractions, respectively. On average, the PM10–2.0 size fraction consisted of 49% crustal matter, 30% OM, 4.7% nitrate, 4.4% sulphate, 2.4% sea salt, 1.7% EC, and 0.8% ammonium by mass. In the PM2.0 size fraction, OM made up 43%, EC 21%, crustal matter 14%, sulphate 13%, nitrate 5.8%, and ammonium 5.7% of the particulate mass (Maenhaut et al., 2005). The objectives of the present paper are to report and interpret the fine structure of the PM and elemental mass size distributions in the aerodynamic diameter (AD) range between about 50 nm and 10 μm, to investigate the temporal variation in the relative contribution of the modes, and to relate the modes to source types and formation mechanisms.

2. Methods

2.1. Aerosol sampling

The aerosol samples were collected during an intensive field campaign on the first-floor balcony at a height of about 7.5 m above the street level at 5, Rákoczi Street in downtown Budapest (Word Geodetic System 1998 coordinates: latitude 47°29′37″N, longitude 19°03′38″E, altitude 111 m above the mean sea level) from 23 April through 5 May 2002. The site can be classified as kerbside according to the criteria proposed by the European Environmental Agency (Larssen and Kozakovic, 2003). It was located within a street (urban) canyon that is characterised by a length of approximately 600 m, a width of 25–40 m, and a typical height of 25–30 m. The street and its actual section belong to regular street canyons within which air pollution build-up is favoured (Hunter et al., 1992). The mean number of motor vehicles passing the street in both directions per 15 min was obtained on line from loop counting, and ranged from 86 to 766 with an overall mean of 513.

Among the cascade impactor devices deployed was a micro-orifice uniform deposit impactor (MOUDI, Marple et al., 1991) for measuring the PM mass size distribution. It has 11 impaction stages and a backup filter stage. The cut-off ADs for the impaction stages are 18, 9.9, 6.2, 3.1, 1.8, 1.0, 0.603, 0.301, 0.164, 0.094, and 0.053 μm (numbered 0–10). The device operates at a flow rate of $30\,l\,min^{-1}$, and the samples were collected on ungreased 37 mm diameter aluminium foils ($4\,mg\,cm^{-2}$) for the impaction stages and on double Whatman QM-A quartz fibre backup filters. The foils and filters had been pre-heated at 550 °C to remove organic contaminants prior to sampling. The MOUDI had no additional inlet. Use was also made of a small deposit area low-pressure impactor (SDI, Maenhaut et al., 1996) for measuring elemental mass size distributions. It has 12 impaction stages with cut-off ADs of 8.50, 4.08, 2.68, 1.66, 1.06, 0.796, 0.591, 0.343, 0.231, 0.153, 0.086, and 0.045 μm (numbered 12–1), and was equipped with an upper size AD cut-off inlet of 15 μm. The device operates at a flow rate of $11\,l\,min^{-1}$, and the samples were collected on 1.5 μm thick Kimfol polycarbonate film. In order to reduce particle bounce-off effects, the films were coated with vaseline for stages 12–6, and with paraffin for stages 5–1. The SDI has an improved size resolution for submicrometer particles, enabling to resolve typical atmospheric aerosol size distributions in this range; and the smallest cut-off value of the stages makes it possible to detect even the Aitken mode particles, which are believed to play an important role in the aerosol formation processes. The collection efficiency for each stage of the SDI was calibrated (Hillamo and Kauppinen, 1991; Maenhaut et al., 1996) with monodisperse aerosols, while the collection efficiency curves for the MOUDI were supplied by the manufacturer, and were adjusted (fine-tuned) according to their experimentally determined 50% cut-off values. The devices were operated in parallel with their inlets facing up, and the aerosol samples were collected separately over daytime periods (7:00–19:00 local daylight saving time) and nights (19:30–6:30). A total of 11 samples for daytime periods, and 12 samples for night

periods (labelled as N1, D2, N2,…, D12, N12) together with 6 field blank samples were obtained. The samples were placed into polycarbonate petri slide dishes; the MOUDI stages were frozen at −25 °C during transport and storage, the SDI stages were stored at a temperature of 2–4 °C. In the present paper, use is also made of some complementary atmospheric concentrations for impactor data validation purposes, obtained from parallel collections by stacked filter unit (SFU) samplers on nuclepore filters. More information on the SFU sampler, actual collections, and analyses can be found, e.g., in Maenhaut et al., (2005); and Salma et al., (2004).

The first 5 days of the campaign were characterised by changing, cloudy, and more wet weather conditions which were finished by a cold front that passed the city on 27 April. Over the last 7 days, the weather was generally more stable, dry, and warm with clear sky. In the first period, the atmospheric concentrations were generally smaller than in the second period, and the mean values were changing irregularly from day to day, but were usually larger for the daylight periods than for the nights. In the second period the wind speed was lower, the atmospheric concentrations were generally larger, and had increasing tendency. The build-up of the mean concentrations continued monotonically even from daytime period to night (Salma et al., 2004).

2.2. Chemical analyses and data treatment

Aerosol mass was obtained from the MOUDI samples by weighing each collection substrate before and after sampling with a microbalance with a sensitivity of 1 μg. The substrates were pre-equilibrated before actual weighing at a temperature of 20 °C and relative humidity of 50% for at least 24 h. The SDI samples were analysed for 29 elements (i.e., Na, Mg, Al, Si, P, S, Cl, K, Ca, Ti, V, Cr, Mn, Fe, Ni, Cu, Zn, Ga, Ge, As, Se, Br, Rb, Sr, Zr, Nb, Mo, Ba, and Pb) by particle-induced X-ray emission (PIXE) analysis at the Ghent University (Maenhaut et al., 1996; and references cited therein). Field blank correction was applied to both data sets.

The experimental results were inverted into smooth size distributions by the computer program MICRON (Wolfenbarger and Seinfeld, 1990). MICRON makes use of the actual collection efficiency curves of the individual impactor stages to construct response (or kernel) functions for the stages and these are then employed together with the experimental data in the inversion. The inversion is based on constrained regularisation and produces a smooth size distribution, which consists of 80 data points (logarithmic size channels). The inverted data were then fitted by log-normal distributions (Winklmayr et al., 1990; Heintzenberg, 1994; Havránek et al., 1996) so that the mass concentrations, geometric mean aerodynamic diameters (GMADs), and geometric standard deviations (GSDs) of the different contributing modes could be obtained for each size distribution. The relative standard deviation derived for the chemical analyses (due to counting statistics and spectrum deconvolution in PIXE) typically ranged from about 1% to 10%. The aerosol sampling in general is expected to introduce an additional relative uncertainty of about 6–8% (Salma et al., 2004); from a number of parallel samplings with two SDI devices (Maenhaut et al., 1999), it can be estimated that the uncertainty due to sampling is around 10% for the SDI stages. Therefore, the analytical standard deviations of the concentration data were increased by a relative uncertainty of 10% quadratically summing them in order to include the sampling uncertainties as well, and to obtain more realistic overall uncertainties. These values were finally utilised as input standard deviations. The effect of input uncertainties on the inverted distributions was tested, and it was found that the peaks in the distributions became broader and slightly smaller with increasing input uncertainty, but that the mode concentrations and GMADs are preserved (Kerminen et al., 1997). The increased uncertainty can, however, disadvantageously affect the detection of modes with very small concentrations, in particular of the Aitken mode. Generally, the experimental data were fitted by three separate modes at most. In a few cases, for S, K, Zn, and the PM, four modes had to be allowed in order to avoid systematic differences in the residuals, and hence in order to better reproduce the experimental data. In such cases, however, the existence of the fourth mode could also be clearly judged by the visual inspection of the raw size distribution data (see Fig. 6). The quality of the fit was usually good or very good (reduced $\chi^2 \approx 1$). In some particular cases, usually at the ends of the size interval investigated, the agreement between the experimental data points and the fitted curve was less perfect, most likely because of other possible modes overlapping from outside the size range studied, due to some distortion in the shape of large (single) peaks, to the shift of the modes during the sampling periods (e.g., with changing relative humidity), and/or to possible sampling errors (bounce-off effects). The uncertainty in the mode diameters obtained by the log-normal fittings is estimated to be typically one channel width of the MICRON inverted size distribution; this corresponds to about 10%, relatively. The individual modal parameters were averaged for each mode and species for all samples, and for separate subgroups of samples representing daytime periods and nights.

3. Results and discussion

3.1. Data validation for cascade impactors

Atmospheric concentrations derived from parallel cascade impactor (SDI and MOUDI) and filter-based

(SFU) samplings were intercompared in order to perform the data validation for the impactor samples. The SFU collects aerosol particles in a PM10–2.0 and a PM2.0 size fraction. The analytical results for them were obtained by a combination of instrumental neutron activation analysis (INAA) and PIXE, and the procedures are quality controlled on a sample by sample basis (Salma et al., 1997). Atmospheric concentrations of several aerosol species for the SFU were given elsewhere (Maenhaut et al., 2005). Atmospheric concentrations of elements from the SDI were summed up for stages 1–9 in order to obtain the concentrations for the PM2.68 size fraction, and these were compared to the PM2.0 concentrations derived from the SFU sampler. Similarly, atmospheric mass concentrations of PM from the MOUDI were summed up for stages 2–10, and for the front backup filter in order to get the masses for the PM9.9 size fraction, and these were compared to the PM10 masses from the SFU sampler (obtained by adding data for the PM 10–2.0 and PM2.0 size fractions). The mean SDI/SFU concentration ratio for elements listed in Table 1 and for the fine size fractions mentioned ranged from 0.86 to 1.21 with an overall mean ratio and standard deviation of 1.03 ± 0.10. Sodium and Br were excluded from the averaging because of the systematic differences between the two analytical methods (PIXE and INAA) used for measuring them in SDI and SFU samples (Salma et al., 1997). Sodium data obtained by PIXE tend to be systematically smaller than those obtained by INAA due to difficulties in correcting for the attenuation of the soft Na K X-rays in PIXE and to uncertainties in the background subtraction in that region of the PIXE spectrum; while the halogens, and in particular Br, can be volatilised during the PIXE bombardment in the vacuum. Chlorine was also excluded from the averaging; the SDI/SFU fine ratio for this element was, on average, 2.2 ± 0.8; the Cl on the PM2.0 filter of the SFU is much more prone to losses during sampling from reactions with acidic species than the Cl in the impactor stages (Maenhaut et al., 1987). For the particulate mass, the mean MOUDI/SFU ratio and standard deviation for the PM10 size fraction were 0.78 ± 0.08. This somewhat smaller than 1.0 ratio can be explained by wall losses in the impactor (ungreased aluminium impaction foils were used in the MOUDI), perhaps to a smaller extent also by some systematic inaccuracies in the volume measurements of the two samplers, by possible inaccuracies in the upper cut-off values of the two samplers, and by difficulties in gravimetric mass determination for the lightly loaded impactor stages. Similar elemental and PM mass concentration ratios were obtained in other intercomparisons (Maenhaut et al., 1999). Nevertheless, very strong correlations between the summed cascade impactor data (PM2.68 size fraction for the elements, and PM9.9 size fraction for the aerosol mass) and the SFU

Table 1
Average geometric mean aerodynamic diameter (GMAD), number of occurrence (No.) in 23 samples, and relative mode concentration (RMC) for the two accumulation submodes, intermediate, and coarse modes, and for 15 selected elements and the PM in downtown Budapest in spring 2002

Species	Accumulation 1 mode			Accumulation 2 mode			Intermediate mode			Coarse mode		
	GMAD (μm)	No.	RMC (%)	GMAD (μm)	No.	RMC (%)	GMAD (μm)	No.	RMC (%)	GMAD (μm)	No.	RMC (%)
Al		0			0		0.94	11	4	4.5	23	96
Si		0			0		0.96	15	4	4.7	23	96
Ca		0			0		0.96	14	4	4.8	23	96
Ti		0			0		0.90	17	4	4.8	23	96
Fe		0			0		0.90	22	7	4.1	23	93
Cl	0.39	21	10		0		1.2	18	14	4.6	23	76
Zn	0.29	23	12		0		0.87	23	29	4.4	23	59
Na	0.34	23	15	0.79	17	26		0		3.3	23	58
Mn	0.29	18	5	0.76	23	13		0		3.9	23	83
Ni	0.29	23	19	0.76	21	11		0		4.0	23	69
Cu	0.31	14	5	0.79	21	10		0		3.7	23	85
Pb	0.26	23	28	0.68	23	41		0		3.3	23	31
K	0.31	23	19	0.71	21	12	2.2	7	13	4.6	23	55
S	0.30	23	46	0.59	22	42		0		3.9	19	12
Br	0.32	23	55	0.63	16	26		0		3.8	23	19
PM	0.27	23	26	0.65	11	27	2.6	22	20	8.6	23	27

For the GMADs, the uncertainty in the individual data is estimated to be about 10% and the relative standard deviation, as calculated from the spread in the individual data for a mode of an element, was about 12%. For the RMCs (with value $>20\%$), the uncertainty in the individual data is estimated to be smaller than 17%.

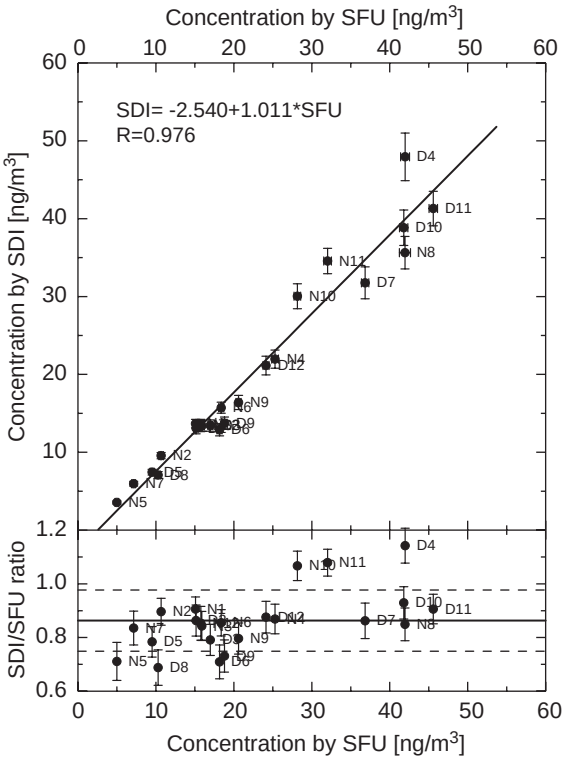

Fig. 1. Scatter plot of atmospheric concentrations in the PM2.68 and PM2.0 size fractions derived from the SDI and SFU samplers, respectively, and SDI/SFU concentration ratios for Cu. The error bars indicate ±1 standard deviation of the analytical results; the mean SDI/SFU ratio and its standard deviation of 0.86±0.11 are indicated by the solid and dashed lines, respectively, on the bottom panel.

concentrations (PM2.0 for the elements, and PM10 for the aerosol mass) were obtained within the range of 0.91 (for K) and 0.98 (for Ni) with an overall mean correlation coefficient of 0.96±0.02. Sodium, Cl and Br were excluded from averaging again. The comparison for Cu is displayed in Fig. 1. The ratios indicated good consistency between the data sets from the cascade impactors and the SFU sampler, and confirmed that the losses from the lower stages of the impactors during the samplings do not seem to be serious.

3.2. Fine structure of mass size distributions

Average GMAD, number of occurrence in 23 samples, and the relative mode concentration (RMC) for 15 selected elements and the PM are presented in Table 1. It is seen that the size distributions in the size interval investigated were made up of several modes. For the elements Al, Si, Ca, Ti, and Fe, the size distributions generally consisted of a large coarse mode with a GMAD of 4–5 μm containing about 96% of the elemental mass, and of a smaller but unambiguously present mode (called here intermediate mode) with a GMAD at about 1 μm containing only 4% of the elemental mass, on average. Typical GSDs of the modes were between 1.8–2.0 and 1.4–1.7, respectively. The intermediate mode was missing for some samples. Similar doublets of modes (called lower and upper coarse modes) were observed at an urban site in Helsinki, whereas the lower coarse mode was missing in the rural samples collected in parallel (Pakkanen et al., 2001), and in the UK for Fe and Ba (Allen et al., 2001). The two modes for Fe are shown in Fig. 2 as an example, and the map of individual mode concentration as function of GMAD for Si is displayed in Fig. 3. The coarse mode is mainly associated with particles from local origin (Salma et al., 2004; Maenhaut et al., 2005) generated by both natural processes (erosion, wind dispersed road, and soil dust) and anthropogenic activities (e.g., thermal- and motion-induced mobilisation of road dust, frictional emissions from mechanical components of vehicles such as tires and brakes). Correlation between the coarse-mode concentration pairs of the typical crustal elements (i.e., Al, Si, Ca, Ti, Mn, and Fe) was strong, as expected, and the correlations in the set including in addition coarse S, K, Br, Pb, and PM resulted in coefficients (R) between 0.8–0.9. The strong correlation supports the idea that the main source for these components, most likely suspension and resuspension, is common. Fig. 3 also shows that the GMADs were spread in a relatively small interval, that no systematic relationship was observed between GMAD and corresponding mode concentration, and that there was no significant correlation between the two sets of modal concentrations, and of GMADs. The mean correlation coefficients between the coarse and intermediate mode concentrations and between the GMADs of the coarse and intermediate modes, for the crustal elements listed above and PM, were typically 0.69±0.17 (moderate correlation) and 0.31±0.23 (negligible correlation), respectively. Crustal enrichment factors for intermediate mode concentrations, calculated relative to Mason's average crustal rock composition (Mason and Moore, 1982) with Al as reference element, were similar to those in the coarse mode, and to the values derived for the whole coarse size fraction. This indicates that these particular elements in the intermediate mode were also attributable to crustal sources, which can, however, be different from those for the coarse mode. One example of such a source is emissions of fly ash from coal combustion (containing silica, alumina, Fe, and Ca oxides); the intermediate mode may consist of particles of regional origin as well. It has to be noted that the mean correlation coefficient between the pairs of the intermediate mode concentrations of the crustal elements and PM was typically 0.60±0.20 only,

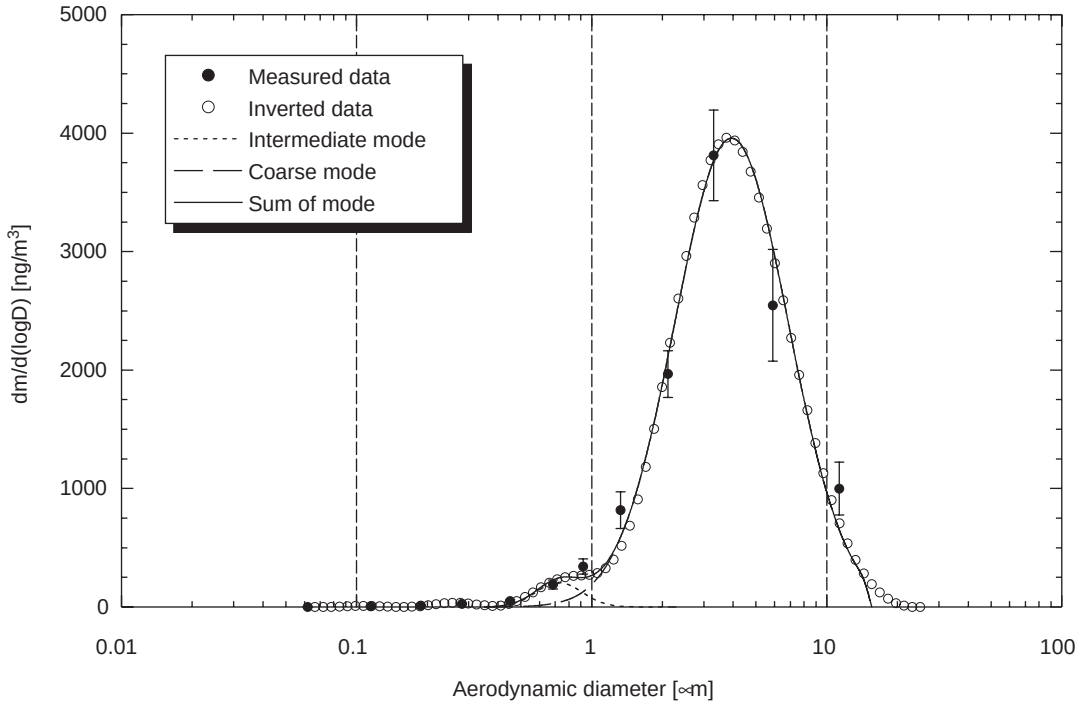

Fig. 2. Mass size distribution of Fe in downtown Budapest for the daytime period on 29 April 2002. The error bars indicate ± 1 standard deviation. The atmospheric concentrations in the intermediate and coarse modes were 51 and 2400 ng m^{-3}, respectively, and the GMADs for the two modes were 0.73 μm (GSD: 1.3) and 3.9 μm (GSD: 1.7), respectively.

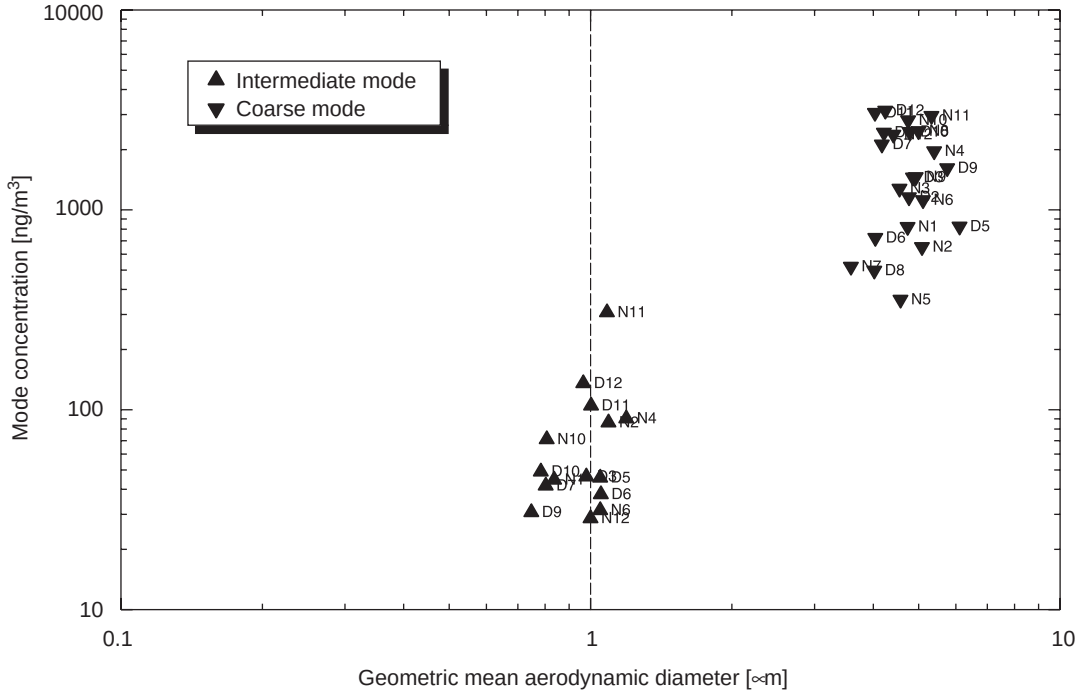

Fig. 3. Geometric mean aerodynamic diameters as function of modal concentration for Si in downtown Budapest in spring 2002.

thus similar to the correlation coefficient between the coarse and intermediate concentrations. The correlation between the GMADs of the intermediate mode for the crustal elements was stronger, with a mean coefficient of 0.73 ± 0.11. An alternative explanation for the intermediate mode could reside in the production mechanisms of the mineral aerosol from the road dust. Some wind tunnel experiments (Alfaro et al., 1998), mathematical models (Alfaro and Gomes, 2001), and field measurements (Clarke et al., 2004) suggest that the atmospheric mineral aerosol released by saltation processes in mineral dust source regions can always be considered as a mixture of three populations (modes) with geometric mean diameters of 1.1–1.5, 5.5–6.7, and 14–19 μm, respectively. The relative intensities of the three modes depend mainly on the wind speed and binding energy in the target soil. The coarsest of these three modes lies outside the AD interval studied, but the other two modes with the smaller diameters could, at least in principle, correspond to the coarse and intermediate modes observed in the present work. However, the correlation between the coarse-to-intermediate concentration ratio and the wind speed (both within the street canyon and above the rooftop level) was not significant, and the real physical conditions in urban environments are certainly different from those for the saltation process in source regions of natural mineral dust. In conclusion, more research will be needed to arrive at a firm identification of the origin and sources of the intermediate mode.

For the elements Cl, Zn, Na, Mn, Ni, Cu, Pb, S, and Br, the distributions were generally trimodal (as an example, a trimodal distribution for Ni is shown in Fig. 4); they contained a coarse mode and separate submicrometer-sized submodes (instead of a single accumulation mode). Also the PM often exhibited two separate submodes in the submicrometer size range; the upper of these two modes was only observed in half of the samples, though; the fact that the MOUDI has fewer impaction stages in the submicrometer size range than the SDI makes it more difficult to resolve the submicrometer-sized modes. The mode diameter for the upper of the two submodes of the elements Cl and Zn was larger than that of the other elements; it was actually similar to that of the intermediate mode of the crustal elements and was therefore placed in the "Intermediate mode" column in Table 1. Furthermore, the mode diameter for the upper of the two submodes is clearly lower for S, Br, and the PM than for the other elements, suggesting different sources and/or source processes. Two submicrometer submodes were observed earlier for particulate sulphate, ammonium, and nitrate

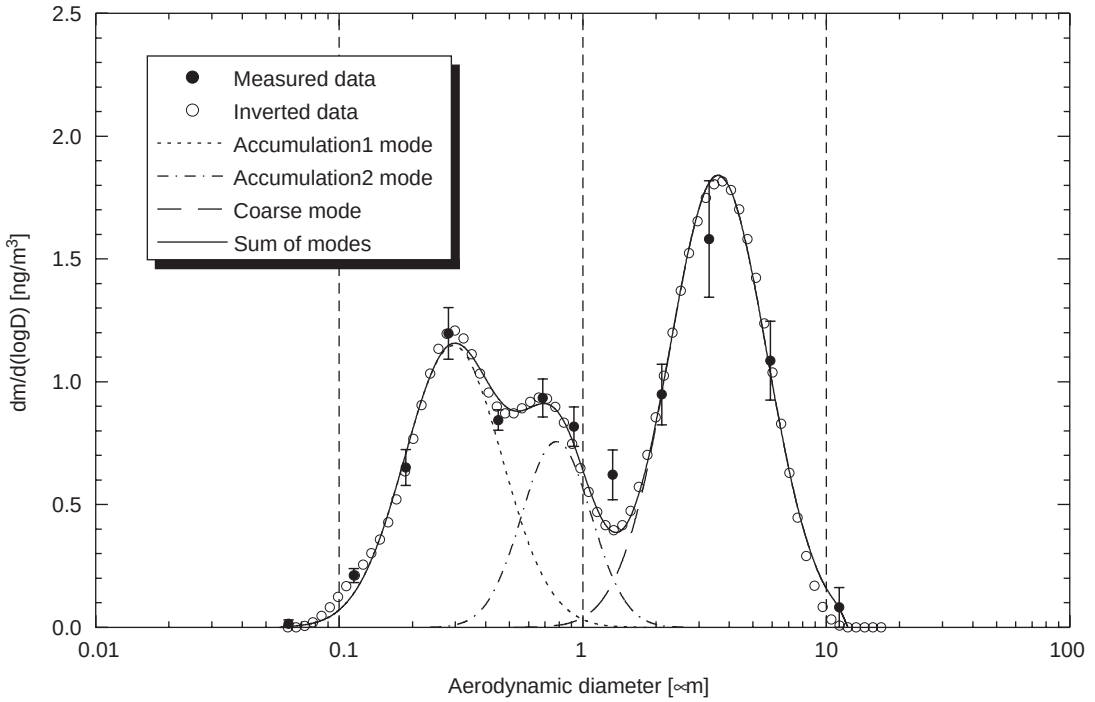

Fig. 4. Mass size distribution of Ni in downtown Budapest for the daytime period on 25 April 2002. The error bars indicate ± 1 standard deviation. The atmospheric concentrations in the accumulation 1, accumulation 2, and coarse modes were 0.57, 0.27, and 0.93 ng m^{-3}, respectively, and the GMADs for the three modes were 0.30 μm (GSD: 1.4), 0.78 μm (GSD: 1.4), and 3.6 μm (GSD: 1.6), respectively.

(Hering and Friedlander, 1982; John et al., 1990; Hering et al., 1997), and were labelled as condensation and droplet modes. The formation of the droplet mode is explained by the activation of condensation mode particles to form fog or cloud drops followed by aqueous-phase chemistry and fog or cloud evaporation (Meng and Seinfeld, 1994; Kerminen and Wexler, 1995). The upper submicrometer mode for S and possibly also for Br (and to some extent also for the PM) most likely corresponds to the droplet mode of the earlier studies and has the same formation process. It is interesting to note in this respect that the ratio of the droplet mode to the condensation mode mass concentration was typically a factor of 1.5 larger during the first 5 cloudy days of the campaign than during the last 7 dry days. Cloud or fog processing can hardly be invoked for the upper submicrometer mode of the metallic elements, as these elements are less water-soluble, their mode diameter is larger than that of S, and the sources are most likely more local (vs more regional for S), so that there is insufficient time for such processing. Multiple modes in the submicrometer size range for the metallic elements have also been seen in previous studies (e.g., Dodd et al., 1991; Allen et al., 2001). The lower of our two submicrometer modes for the metallic elements is likely mainly due to condensation processes (as is also the case for S), whereas the upper one probably originates from a variety of high-temperature dispersion and abrasion processes. The relative intensities (RMC-values in Table 1) of the two submicrometer modes and the coarse mode of the elements Cl, Zn, Na, Mn, Ni, Cu, Pb, S, and Br varied substantially from element to element. On average, more than half of the elemental mass for Cl, Zn, Na, Mn, Ni, and Cu was observed in the coarse mode, which indicates that their main source processes are disintegration and dispersion, resuspension of surface dust, or abrasion mechanisms (Salma et al., 2002; Maenhaut et al., 2005). This is illustrated in Fig. 5 by the map of individual modal concentrations as function of GMAD for Cu. Automotive break wear emissions are an important source for Cu and Zn (and also for Pb); for Zn, tire wear is an important additional source (Weckwerth, 2001; Pakkanen et al., 2003; Lough et al., 2005). In the recent study of Lough et al. (2005) on the emissions of metals associated with motor vehicle roadways, which was performed in two tunnels, multimode mass size distributions were observed for Cu, Pb, and Zn, which show some resemblance to these obtained in this work. The coarse mode was the major one for the three elements in that study and it was attributed to the emission of roadway dust that was enriched with particles from break and tire wears. As indicated above, the RMCs of the three modes for the anthropogenic elements varied substantially from element to element. In addition, there was quite some sample-to-sample variability in the RMCs of the modes for each element

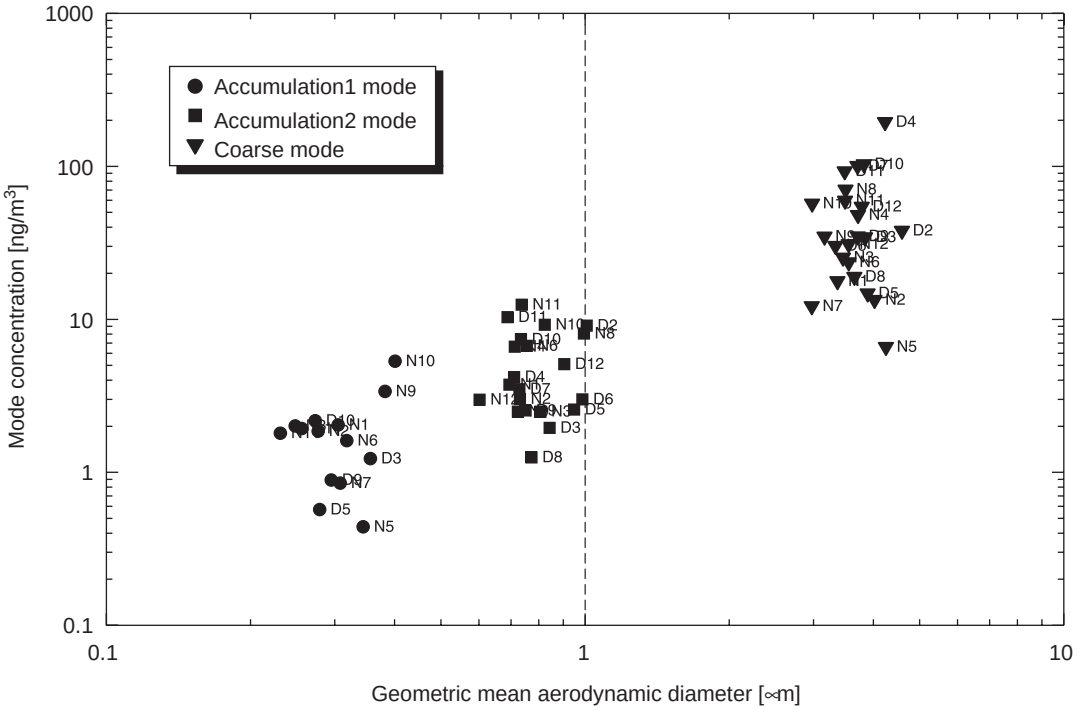

Fig. 5. Geometric mean aerodynamic diameters as function of modal concentration for Cu in downtown Budapest in spring 2002.

and the mode diameters of the upper submicrometer mode were not the same for all elements. All this points to multiple sources and/or source processes for the anthropogenic elements listed.

For K, altogether four modes were detected in the size distributions, but the intermediate mode had a significantly larger mean GMAD of 2.2 μm than the other elements (which had a GMAD of about 0.9 μm). With regard to the PM mass, in addition to the two submicrometer modes, also two supermicrometer modes were observed. The relative intensities of the coarse and two submicrometer modes were practically equal, while the contribution of the intermediate mode was somewhat smaller. The GMAD for the lower accumulation mode (denoted as accumulation1 in Table 1) of the PM tended to increase with mode concentration (or relative mode concentration, correlation coefficient 0.75), and a similar, but weaker correlation was observed for the elements. It should be noted that the GMADs for the coarse and intermediate modes of the PM mass were larger than expected on the basis of the elemental GMAD values. Possible explanations for this discrepancy are inaccuracies in the cut-off diameters for the first few stages of the SDI and/or MOUDI impactors used (Maenhaut et al., 1999), the fact that different inlets were employed, and interstage losses (bounce-off effects). It has also to be noted that the detailed size distributions of the carbonaceous aerosol in particular and of nitrate, which together made up about 35% of the aerosol mass in the PM10–2.0 size fraction (Maenhaut et al., 2005), were not determined, but also affected the size distribution of the PM.

On the basis of several previous studies (e.g., Berner et al., 2004), it was expected that an Aitken mode (with a GMAD $< \approx 0.15$ μm) would be detected in the mass size distributions for our environment which is very strongly influenced by road traffic. The distributions, however, did not confirm this anticipation; the Aitken mode was observed only as an exception for S, K, and Zn (see Fig. 6 as an example) but, in general, it was missing. This finding is in accordance with the results for a freeway-influenced aerosol (Morawska et al., 1999). The elemental mass contained in the Aitken mode was usually only a few ng m^{-3}, which is negligible compared to that in the other modes.

3.3. Daytime period and night differences

Atmospheric concentrations of the elements and PM in the coarse mode were usually smaller over nights than over daytime periods, on average by 10–15%. This points to the significance of the local dust mobilisation

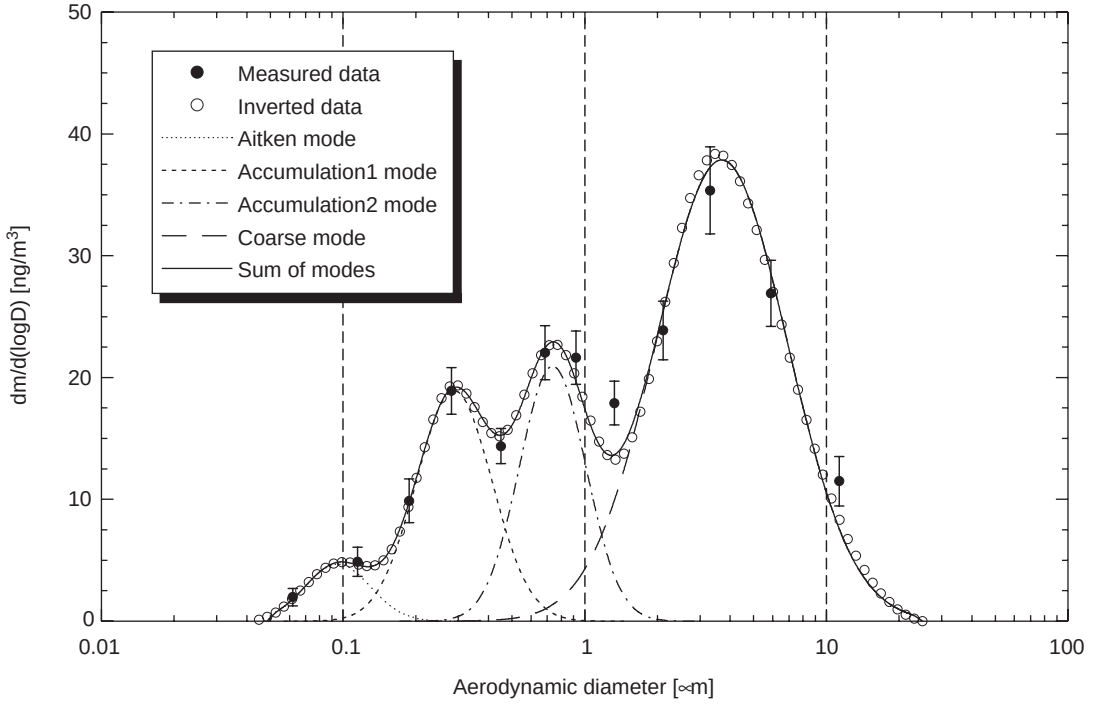

Fig. 6. Mass size distribution of Zn in downtown Budapest for the night on 25 April 2002. The error bars indicate ±1 standard deviation. The atmospheric concentrations in the Aitken, accumulation 1, accumulation 2, and coarse modes were 1.6, 7.4, 8.7, and 26 ng m^{-3}, respectively, and the GMADs for the four modes were 0.10 μm (GSD: 1.4), 0.29 μm (GSD: 1.4), 0.74 μm (GSD: 1.4), and 3.7 μm (GSD: 1.8), respectively.

and resuspension processes for the coarse mode, and to the short atmospheric residence time for the coarse particles. The elements S, Ca, Cu, and Zn for the coarse mode exhibited an even smaller mean night-to-daytime-period concentration (N/D) ratio of about 0.7–0.8. The main source for the latter elements is vehicular traffic: mechanical wear of tires (for S and Zn), of brake linings (for Cu), and lubricating engine oil (for Ca), which is linked firstly to daytime periods (Weckwerth, 2001; Pakkanen et al., 2003). (The mean N/D ratio for the vehicular circulation was 0.38.) It is worth noting that the actual change in the intensity of the emission sources from daytime periods to nights could even be larger than that inferred from the concentration ratios because its real effect is partly counterbalanced by decrease of the mixing height from daytime periods to nights. The number of data available for the intermediate mode was rather limited; nevertheless, the concentrations in the intermediate mode seemed to be usually larger over nights than over daytime periods by about 20–40%, which seems to suggest an anthropogenic and regional origin. For intermediate-mode K, N/D ratios were smaller than one, which suggests that it had different source type(s) than the other elements. For intermediate-mode PM, no significant difference between daytime periods and nights was observed. The N/D ratio for the upper accumulation mode of the elements and PM changed irregularly between 0.6 and 1.4. There was no systematic difference in the lower accumulation mode of the PM between daytime periods and nights.

The GMADs of the elements and PM for the two accumulation modes tended to shift to somewhat larger values over nights than over daytime periods, presumably due to larger ambient relative humidity during night (on average 80% vs. 68% during daytime) and associated hygroscopic growth. In contrast, the GMAD for the coarse-mode PM appeared to shift to lower values over nights than during daytime periods, possibly as a result of lower wind speed and less traffic during the night. For the coarse mode of the various elements studied, no significant change in GMAD from daytime period to night was seen.

4. Conclusions

The cascade impactors with enhanced size resolution and the inversion algorithm used jointly in the present study were shown to be valuable and efficient tools for deriving and investigating the fine structure of the mass size distributions of the atmospheric aerosol and its constituents. The resulting quasi-continuous size distributions displayed a clear modal structure, which is consistent with our understanding of the main emission sources and mechanisms. By evaluating the mass size distributions in detail, an additional (intermediate) mode located at about 1 μm AD was identified for the typical crustal elements; this finding confirmed an earlier observation in an urban environment. The intermediate mode could be related to fly ash from coal burning in the region, but road dust dispersal may also have in part contributed to it. In the submicrometer size range two different submodes were observed, with the lower one centred at 0.31 ± 0.03 μm AD. The mode diameter for the upper submode was somewhat lower for S, Br, and the PM than for the other elements (i.e., about 0.60 μm vs. about 0.75 μm), suggesting different sources and/or source processes. The variation in the overall size distributions and RMCs for the various elements indicated the existence of multiple sources, including vehicular (both combustion and frictional) and industrial emissions, resuspension of road and soil dust, and long-range transport of air masses. The significant coarse mode for some typical anthropogenic elements (Cu and Zn) and the observed coarse mode concentration differences between daytime periods and nights (e.g., for Ca) point to the importance of frictional sources and road dust resuspension in cities, which are both primarily related to road traffic.

Acknowledgement

Financial support by the Hungarian Scientific Research Fund (contr. T043348); by the Special Research Fund of Ghent University, by a bilateral project between Hungary and Flanders, and by the Belgian Federal Science Policy Office (contrs. EV/02/11A and BL/02/CR01) is appreciated. The authors are indebted to J. Cafmeyer and S. Dunphy for technical assistance.

References

Alfaro, S.C., Gomes, L., 2001. Modelling mineral aerosol production by wind erosion: emission intensities and aerosol size distributions in source areas. Journal of Geophysical Research 106, 18075–18084.

Alfaro, S.C., Gaudichet, A., Gomes, L., Maillé, M., 1998. Mineral aerosol production by wind erosion: aerosol particle sizes and binding energies. Geophysical Research Letters 25, 991–994.

Allen, A.G., Nemitz, E., Shi, J.P., Harrison, R.M., Greenwood, J.C., 2001. Size distribution of trace metals in atmospheric aerosol in the United Kingdom. Atmospheric Environment 35, 4581–4591.

Balásházy, I., Hofmann, W., Heistracher, T., 2003. Local particle deposition pattern may play a key role in the development of lung cancer. Journal of Applied Physiology 94, 1719–1725.

Berner, A., Galambos, Z., Ctyroky, P., Frühaus, P., Hitzenberger, R., Gomišček, B., Hauck, H., Preining, O., Puxbaum, H., 2004. On the correlation of atmospheric

aerosol components of mass size distributions in the larger region of a central European city. Atmospheric Environment 38, 3950–3970.

Clarke, A.D., Kapustin, V.N., Shinozuka, Y., Howell, S., Huebert, B., Masonis, S., Anderson, T., Covert, D., Weber, R., Anderson, J., Zin, H., Moore II, K.G., McNaughton, C., 2004. Size-Distributions and mixtures of dust and black carbon aerosol in Asian outflow: physio-chemistry and optical properties. Journal of Geophysical Research 109, doi:10.1029/20003JD004378.

Crutzen, P., 2004. New directions: the growing urban heat and pollution "island" effect—impact on chemistry and climate. Atmospheric Environment 38, 3539–3540.

Dodd, J.A., Ondov, J.M., Tuncel, G., Dzubay, T.G., Stevens, R.K., 1991. Multimodal size spectra of submicrometer particles bearing various elements in rural air. Environmental Science and Technology 25, 890–903.

Havránek, V., Maenhaut, W., Ducastel, G., Hanssen, J.E., 1996. Mass size distributions for atmospheric trace elements at the Zeppelin background station in Ny Ålesund, Spitsbergen. Nuclear Instruments and Methods B 109/110, 465–470.

HEI Review Committee (HEI), 2002. Understanding the Health Effects of Components of the Particulate Matter: Progress and Next Steps. Health Effect Institute, Boston.

Heintzenberg, J., 1994. Properties of the log-normal particle size distribution. Aerosol Science and Technology 21, 46–47.

Hering, S.V., Friedlander, S.K., 1982. Origins of aerosol sulfur size distribution in the Los Angeles Basin. Atmospheric Environment 16, 2647–2656.

Hering, S., Eldering, A., Seinfeld, J.H., 1997. Bimodal character of accumulation mode aerosol mass distributions in Southern California. Atmospheric Environment 31, 1–11.

Hillamo, R., Kauppinen, E.I., 1991. On the performance of the Berner low pressure impactor. Aerosol Science and Technology 14, 33–47.

Hillamo, R., Kerminen, V.-M., Aurela, M., Mäkelä, T., Maenhaut, W., Leck, C., 2001. Modal structure of chemical mass size distribution in the high Arctic aerosol. Journal of Geophysical Research 106, 27555–27571.

Hunter, L.J., Johnson, G.T., Watson, I.D., 1992. An investigation of three-dimensional characteristics of flow regimes within the urban canyon. Atmospheric Environment 26, 425–432.

Hussein, T., Puustinen, A., Aalto, P., Mäkelä, J.M., Hämeri, K., Kulmala, M., 2004. Urban aerosol number size distributions. Atmospheric Chemistry and Physics 4, 391–411.

Jacobson, M.Z., 2001. Strong radiative heating due to the mixing state of black carbon in atmospheric aerosols. Nature 409, 695–697.

John, W., Wall, S.M., Ondo, J.L., Winklmayr, W., 1990. Modes in the size distributions of atmospheric inorganic aerosol. Atmospheric Environment 24A, 2349–2350.

Kaufman, Y.J., Tanré, D., Boucher, O., 2002. A satellite view of aerosols in the climate system. Nature 419, 215–223.

Kerminen, V.-M., Wexler, A.S., 1995. Growth laws of atmospheric aerosol particles: an examination of the bimodality of the accumulation mode. Atmospheric Environment 22, 3263–3275.

Kerminen, V.-M., Aurela, M., Hillamo, R.E., Virkkula, A., 1997. Formation of particulate MSA—deductions from size distribution measurements in the Finnish Arctic. Tellus B 49, 159–171.

Larssen, S., Kozakovic, L., 2003. EuroAirnet—Status Report 2000, Technical Report No. 90. European Environmental Agency, Copenhagen.

Lough, G.C., Schauer, J.J., Park, J.S., Shafer, M.M., Deminter, J.T., Weinstein, J.P., 2005. Emissions of metals associated with motor vehicle roadways. Environmental Science and Technology 39, 826–836.

Maenhaut, W., Raemdonck, H., Andreae, M.O., 1987. PIXE analysis of marine aerosol samples: accuracy and artifacts. Nuclear Instruments and Methods in Physics Research B 22, 248–253.

Maenhaut, W., Hillamo, R., Mäkelä, T., Jaffrezo, J.L., Bergin, M.H., Davidson, C.I., 1996. A new cascade impactor for aerosol sampling with subsequent PIXE analysis. Nuclear Instruments and Methods B 109/110, 482–487.

Maenhaut, W., Ptasinski, J., Cafmeyer, J., 1999. Detailed mass size distributions of atmospheric aerosol species in the Negev Desert, Israel, during ARACHNE-96. Nuclear Instruments and Methods B 150, 422–427.

Maenhaut, W., Schwarz, J., Cafmeyer, J., Annegarn, H.J., 2002. Study of elemental mass size distributions at Skukuza, South Africa, during the SAFARI 2000 dry season campaign. Nuclear Instruments and Methods B 189, 254–258.

Maenhaut, W., Raes, N., Chi, X., Cafmeyer, J., Wang, W., Salma, I., 2005. Chemical composition and mass closure for fine and coarse aerosols at a kerbside in Budapest, Hungary, in spring 2002. X-ray Spectrometry 34, 290–296.

Marple, V.A., Rubow, K.L., Behm, S.M., 1991. A Microorifice Uniform Deposit Impactor (MOUDI): description, calibration, and use. Aerosol Science and Technology 14, 434–446.

Mason, B., Moore, C.B., 1982. Principles of Geochemistry, 4th edition. Wiley, New York.

Meng, Z., Seinfeld, J.H., 1994. On the source of the submicrometer droplet mode of urban and regional aerosols. Aerosol Science and Technology 20, 253–265.

Morawska, L., Thomas, S., Jamriska, M., Johnson, G., 1999. The modality of particle size distributions of environmental aerosols. Atmospheric Environment 33, 4401–4411.

Offenberg, J.H., Baker, J.E., 2000. Aerosol size distributions of elemental and organic carbon in urban and over-water atmospheres. Atmospheric Environment 34, 1509–1517.

Pakkanen, T.A., Kerminen, V.-M., Korhonen, C.H., Hillamo, R.E., Aarnio, P., Koskentalo, T., Maenhaut, W., 2001. Use of atmospheric elemental size distributions in estimating aerosol sources in the Helsinki area. Atmospheric Environment 35, 5537–5551.

Pakkanen, T.A., Kerminen, V.-M., Loukkola, K., Hillamo, R.E., Aarnio, P., Koskentalo, T., Maenhaut, W., 2003. Size distribution of mass and chemical components in street-level and rooftop PM1 particles in Helsinki. Atmospheric Environment 37, 1673–1690.

Penner, J.E.P., Dong, X., Chen, Y., 2004. Observational evidence in radiative forcing due to the indirect aerosol effect. Nature 427, 231–234.

Pope III, C.A., Burnett, R.T., Thun, M.J., Calle, E.E., Krewski, D., Ito, K., Thurston, G.D., 2002. Lung cancer,

cardiopulmonary mortality, and long-term exposure to fine particulate air pollution. Journal of American Medical Association 287, 1132–1141.

Salma, I., Maenhaut, W., Annegarn, H.J., Andreae, M.O., Meixner, F.X., Garstang, M., 1997. Combined application of INAA and PIXE for studying the regional aerosol composition in southern Africa. Journal of Radioanalytical and Nuclear Chemistry 216, 143–148.

Salma, I., Maenhaut, W., Zemplén-Papp, É., Záray, Gy., 2001. Comprehensive characterisation of atmospheric aerosols in Budapest, Hungary: physicochemical properties of inorganic species. Atmospheric Environment 35, 4367–4378.

Salma, I., Maenhaut, W., Záray, Gy., 2002. Comparative study of elemental mass size distributions in urban atmospheric aerosol. Journal of Aerosol Science 33, 339–356.

Salma, I., Chi, X., Maenhaut, W., 2004. Elemental and organic carbon in urban canyon and background environments in Budapest, Hungary. Atmospheric Environment 38, 27–36.

Singh, M., Jaques, P.A., Sioutas, C., 2002. Size distribution and diurnal characteristics of particle-bound metals in source and receptor sites of the Los Angeles Basin. Atmospheric Environment 36, 1675–1689.

Talukdar, S.S., Swihart, M.T., 2003. An improved data inversion program for obtaining aerosol size distribution from scanning differential mobility analyzer data. Aerosol Science and Technology 37, 145–161.

Vignati, E., Berkowicz, R., Palmgren, F., Lyck, E., Hummelshøj, P., 1999. Transformation of size distributions of emitted particles in streets. The Science of the Total Environment 235, 37–49.

Weckwerth, G., 2001. Verification of traffic emitted aerosol components in the ambient air of Cologne (Germany). Atmospheric Environment 35, 5525–5536.

Wehner, B., Wiedensohler, A., 2003. Long term measurements of submicrometer urban aerosols: statistical analysis for correlations with meteorological conditions and trace gases. Atmospheric Chemistry and Physics Discussions 3, 867–879.

Winklmayr, W., Wang, H.-C., John, W., 1990. Adaptation of the Twomey algorithm to the inversion of cascade impactor data. Aerosol Science and Technology 13, 322–331.

Wolfenbarger, J.K., Seinfeld, J.H., 1990. Inversion of aerosol size distribution data. Journal of Aerosol Science 21, 227–247.